

A Numerical Model of Cumulus Dynamics and Microphysics¹

ALAN I. WEINSTEIN²

The Pennsylvania State University, University Park

(Manuscript received 1 July 1969, in revised form 14 October 1969)

ABSTRACT

A one-dimensional, time-dependent numerical model of cumulus convection is presented. The model considers the processes of horizontal mixing, evaporation, precipitation generation and freezing, as well as the standard thermodynamic and dynamic processes in isolated cumuli. The initial calculations show that: 1) the vertical velocity and liquid water content undergo coupled damped oscillations in time; 2) the rate at which precipitation-sized drops are formed and grow by collection are not sensitive parameters in the amount of rain which falls from the clouds; 3) the amount of liquid water in the form of cloud droplets that must be present in the cloud before a few large drops can be developed is a crucial parameter in determining the amount of rain which falls from the clouds (the higher the threshold cloud liquid water content, the lower the ultimate rainfall amount); and 4) the freezing time and precise ice-nucleation temperature affect the amount of rain that falls from the cloud in a way often very different from the way they affect the cloud-top height.

Trial runs with the model agree well with observations in the two cases tried.

1. Introduction

Numerical models of cumulus clouds have traditionally considered either the dynamics and thermodynamics of these clouds or the evolution of precipitation. Recently, considerable attention is being given to the interaction between the dynamics and thermodynamics and the precipitation in cumuli. This recent work has been possible in part because of bigger and faster computers, but mainly because of the idea of Kessler *et al.* (1962-64) of parametrizing the cloud physics calculations. The first published work which used Kessler's parametrization to investigate the interaction in detail was the paper of Srivastava (1967). The present model is very similar to that of Srivastava, but carries the work a bit further by considering horizontal mixing, evaporation and freezing.

The model is a one-dimensional, time-dependent solution of the first law of thermodynamics, the third equation of motion, and a series of moisture balance relationships. A major advantage of the model is its rapid calculation speed and its small core storage requirements. These features make the model appropriate for numerous numerical experiments which are considerably cheaper and easier to control than similar experiments in the field.

The results of model calculations concerning the interaction between the liquid water and the updraft in the cloud verify the findings of Srivastava; namely, that 1) water loading causes the downdrafts to occur

first near the cloud base and then to spread vertically but never reach the cloud top, and 2) the vertical velocity and liquid water content execute coupled oscillations in time.

The freezing calculations showed that the time of freezing and the ice-nucleation temperature are both important parameters in determining the amount of rain that will fall from cumulus clouds. A very important outcome of the calculations from the standpoint of weather modification verification was that there was not a one-to-one relationship between changes in cloud-top height and changes in precipitation in response to freezing at different times and temperatures.

Sensitivity analysis of the cloud microphysical parameters showed that the most important parameter is one which reflects how long it takes the first large hydrometeors to form. Once the hydrometeors are formed, it does not appear to matter how fast they grow by collection nor how fast new ones are formed.

The model is a combination of a time-dependent version of one similar to that used by Hosler *et al.* (1963) and Simpson *et al.* (1965), and the cloud microphysical parametrization developed by Kessler *et al.* A major advantage of the model is its speed of calculation and storage space requirement, making it appropriate for numerous calculations on the same set of environmental conditions. This enables more planning to be done before elaborate field programs are run.

2. The model

a. Interpolation

The computer program was written to be compatible with a standard radiosonde sounding of pressure (mb),

¹ The work presented here was submitted as a Ph.D. thesis at The Pennsylvania State University.

² Present affiliation: Meteorology Research, Inc., Altadena, Calif.

temperature (°C), and relative humidity (ℳ%) at mandatory and significant levels. The interpolation routine reduces this sounding to one of pressure (db), temperature (°K), and mixing ratio (gm gm⁻¹) at equally spaced vertical grid increments by linear interpolation and the appropriate unit conversions. The mixing ratio is derived by first calculating the saturated mixing ratio from the definition of the mixing ratio and the Magnus formula, and then applying the linearly interpolated relative humidity.

The first level of the interpolated sounding is taken as the cloud base level. The sub-cloud layer is taken to have a dry adiabatic temperature lapse rate and a constant mixing ratio. The value of the sub-cloud mixing ratio is the saturation value at cloud base.

b. Thermodynamics

The thermodynamic calculations are similar to those outlined by Austin and Fleisher (1948). The calculations consider the heat balance in a rising parcel of mass *M* which entrains a mass *dM* of environmental air. This heat balance is described by the first law of thermodynamics as

$$dh = (c_p dT - \alpha dp)M, \tag{1}$$

where *dh* is the heat lost or gained by non-adiabatic processes, and the other terms have their standard meteorological meanings.

The non-adiabatic processes to be considered here are condensation (or sublimation), mixing (both sensible and latent heat transfers), evaporation and freezing. The heat gained by the parcel by condensation or sublimation, (*dh*)_c, is

$$(dh)_c = -LMdq_s,$$

where *dq_s* is the change in saturated mixing ratio as the parcel rises some vertical interval *dz* and *L* is either the latent heat of condensation or sublimation depending upon the process occurring.

While rising, the parcel entrains environmental air of mass *dM* with temperature *T_e* and mixing ratio *q_e*. The mixture reaches some equilibrium temperature which involves a sensible heat transfer, (*dh*)_s, of the form

$$(dh)_s = -c_p(T - T_e)dM,$$

which warms or cools the entrained air.

As a result of entraining non-saturated environmental air, the originally saturated parcel becomes slightly subsaturated. At this point, some of the liquid water that was condensed during the ascent is evaporated to resaturate the mixture. This heat loss, (*dh*)_L, is a latent heat transfer and is given by

$$(dh)_L = -L(q_s - q_e)dM.$$

When the supercooled liquid water in the parcel is frozen, there are two more non-adiabatic heat transfer terms to be considered. The first heat transfer, (*dh*)_f,

is the heat gained due to the release of latent heat of fusion, i.e.,

$$(dh)_f = ML_f Q,$$

where *L_f* is the latent heat of fusion, and *Q* the amount of supercooled water that is frozen in units of grams of water per gram of air.

Before freezing occurs, the liquid water and water vapor in the parcel are in vapor equilibrium at the saturation vapor pressure over a water surface. Immediately after freezing has occurred, a similar equilibrium must be achieved between the newly formed ice and the vapor. Since the saturation vapor pressure over an ice surface is less than that over a water surface at the same temperature and pressure, there must be deposition of vapor onto the ice. The heat gained by the parcel by this deposition, (*dh*)_d, is

$$(dh)_d = ML_s(\Delta q_s)_{w \rightarrow i},$$

where *L_s* is the latent heat of sublimation, and (*Δq_s*)_{w→i} is the difference between the saturation mixing ratio over a water surface and that over an ice surface.

Whenever liquid water is brought to regions of calculation where the air is subsaturated (e.g., above cloud top or below cloud base), the water is evaporated to saturate the air. The heat absorbed from the parcel by this evaporation, (*dh*)_e, is

$$(dh)_e = -ML_c[q_s - q, Q]_{\min}$$

where *L_c* is the latent heat of condensation, and the right-hand term is the minimum of the saturation deficit or the liquid water evaporated.

Substitution of all of the heat transfer terms into (1) and dividing by time *dt* yields

$$\begin{aligned} & \frac{-LMdq_s}{dt} - [c_p(T - T_e) + L(q - q_e)] \frac{dM}{dt} \\ & + \frac{M}{dt} [L_f Q + L_s(\Delta q_s)_{w \rightarrow i}] - \frac{ML_c}{dt} [q_s - q, Q]_{\min} \\ & = \left[c_p \frac{dT}{dt} - \alpha \frac{dp}{dt} \right] M. \tag{2} \end{aligned}$$

The Clapyron equation, along with the definition of mixing ratio and the hydrostatic equation, gives the change in saturation mixing ratio with time, i.e.,

$$\left(\frac{1}{q_s} \right) \frac{dq_s}{dt} = \frac{gw}{RT} + \left(\frac{\epsilon L}{RT^2} \right) \frac{dT}{dt}, \tag{3}$$

where *w* is the vertical velocity of the parcel.

Letting

$$\mu w = \left(\frac{1}{M} \right) \frac{dM}{dt}, \quad \alpha \frac{dp}{dt} = -gw,$$

and substituting (3) into (2) yields

$$\begin{aligned} \frac{dT}{dt} = & -\frac{gw}{c_p} \left(1 + \frac{Lq_s}{RT}\right) - \mu w(T - T_e) - \frac{L}{c_p} \mu w(q_s - q_e) \\ & + \frac{L_f Q}{c_p dt} + \frac{L_s}{c_p dt} (\Delta q_s)_{w \rightarrow i} \Big/ \left(1 + \frac{\epsilon L^2 q_s}{c_p RT^2}\right) \\ & - \frac{L_c}{c_p} \left[\frac{(q_s - q)}{dt}, \frac{Q}{dt} \right]_{\min} \Big/ \left(1 + \frac{\epsilon L^2 q_s}{c_p RT^2}\right), \quad (4) \end{aligned}$$

where L is taken as zero for nonsaturated calculations, L_c as zero for saturated calculations, and L_f and L_s are nonzero only through the levels where freezing is allowed to occur. In the region of the cloud above the freezing level, L is taken as L_s .

c. Dynamics

The third equation of motion can be written as

$$\frac{dw}{dt} = -\frac{1}{\rho} \frac{\partial p}{\partial z} - g - \text{drag}. \quad (5)$$

The drag considered here is that due to the weight of the liquid water present in the parcel, gQ , and the drag from the transfer of vertical momentum from the undiluted parcel to the entrained air, μw^2 .

If it is assumed that there is never any horizontal pressure gradient between the parcels in the cloud and the environment, that the environment is in hydrostatic equilibrium, and that the ideal gas law holds, the third equation of motion can be rewritten as

$$\frac{dw}{dt} = \left(\frac{T_v - T_{ve}}{T_v} - Q \right) g - \mu w^2, \quad (6)$$

where the subscript v refers to the virtual temperature which is related to the unsubscripted temperature by

$$\begin{aligned} T_v &= (1 + 0.61q_s)T, \\ T_{ve} &= (1 + 0.61q_e)T_e. \end{aligned}$$

d. Moisture balance

The change of liquid water content of the rising parcel can be best understood by considering the mass of water substance, F_0 , in the original parcel at time $t=0$, the mass of water substance in the entrained air, F_m , and the mass of water substance at time $t=i+dt$, F_i ; thus,

$$\begin{aligned} F_0 &= M(q+Q), \\ F_m &= dMq_e, \\ F_i &= (M+dM)(q+dq+Q+dQ). \end{aligned}$$

Setting $F_i = F_0 + F_m$, dropping the second-order terms,

and dividing by Mdt , we obtain

$$dQ/dt = -dq/dt - \mu w(q - q_e + Q), \quad (7)$$

where $\mu = (1/M)dM/dz$ and Q is the liquid water condensed in the updraft.

The water condensed in the updraft forms very small droplets which have a negligible terminal velocity and thus are totally carried along by the updraft. This class of water is called cloud water Q_c . In time, due to continued condensation, electrical attraction between small droplets and/or turbulent fluctuations in the supersaturation in the cloud, some of the cloud droplets grow large enough to have an important terminal velocity. These larger drops belong to a class of liquid water called hydrometeor water Q_h . The process by which a few hydrometeors are formed is called conversion. Once some hydrometeors are formed, they fall relative to the updraft (and thus relative to the cloud droplets) and grow further by collection.

Most formulations of how and when a few hydrometeors are formed in the general population of small droplets suggest that the process is fastest when the number of small droplets is large. In the context of the parametrization used here, this means that the conversion process should be delayed until the cloud water content reaches some threshold value a . As the cloud water content passes this threshold, some of this water is converted into hydrometeor water at a constant rate K' . The process is calculated according to

$$\left(\frac{dQ_h}{dt} \right)_{\text{conv}} = - \left(\frac{dQ_c}{dt} \right)_{\text{conv}} = \begin{cases} K'(Q_c - a), & Q_c \geq a \\ 0, & Q_c < a \end{cases} \quad (8)$$

The collection process calculations are founded upon the assumption that the hydrometeors take on the exponential drop size distribution of Marshall and Palmer (1948),

$$N = N_0 e^{-\lambda D}, \quad (9)$$

where N is the number of drops per unit volume per unit drop diameter interval, N_0 is the N for the drop diameter interval starting at $D=0$, and λ a parameter describing the spread of the distribution; and that all of the drops fall at the terminal velocity of the median volume drop diameter D_0 of that distribution. Kessler *et al.* fit the Gunn and Kinzer terminal velocity observation to arrive at the terminal velocity V_T relationship

$$V_T = -130D_0^{1/2} \quad [\text{m sec}^{-1}]. \quad (10)$$

Kessler *et al.* show how the standard continuous collection concepts can be combined with (9) and (10) to give the relationship for the transformation of cloud water into hydrometeor water via collection. Thus,

$$\begin{aligned} \left(\frac{dQ_h}{dt} \right)_{\text{coll}} &= - \left(\frac{dQ_c}{dt} \right)_{\text{coll}} \\ &= 6.96 \times 10^{-4} EN_0^{0.125} \rho^{-0.375} Q_c Q_h^{0.375}, \quad (11) \end{aligned}$$

where E is the mean collection efficiency for hydrometeors collecting cloud droplets.

Using (9) and (10) along with some rough approximations relating the evaporation rate of drops to the diameter of the drops and the saturation deficit, Kessler *et al.* also derive an expression for the rate of evaporation of hydrometeor water,

$$\left(\frac{dQ_h}{dt}\right)_{\text{evap}},$$

of the form

$$\begin{aligned} \left(\frac{dQ_h}{dt}\right)_{\text{evap}} &= -\left(\frac{dq}{dt}\right)_{\text{evap}} \\ &= -1.92 \times 10^6 N_0^{0.35} \rho^{-0.65} (q_s - q_e) Q_h^{0.65}. \end{aligned} \quad (12)$$

Using (7), assuming that the cloud water Q_c is the only liquid water that is evaporated in the entrainment process, the relationship for mixing ratio that is given in (3), and the various moisture transformation processes given above [(8), (11) and (12)], the moisture balance equations can be summarized as

$$\frac{dQ}{dt} = \frac{dQ_c}{dt} + \frac{dQ_h}{dt}, \quad (13)$$

$$\begin{aligned} \frac{dQ_c}{dt} &= \frac{dq_s}{dt} - \mu \bar{w} (q - q_e + Q_c) + \left(\frac{dQ_c}{dt}\right)_{\text{conv}} + \left(\frac{dQ_c}{dt}\right)_{\text{coll}} \\ &\quad - \left[\frac{(q_s - q)}{dt}, \frac{Q_c}{dt} \right]_{\text{min}}, \end{aligned} \quad (13a)$$

$$\frac{dQ_h}{dt} = \left(\frac{dQ_h}{dt}\right)_{\text{conv}} + \left(\frac{dQ_h}{dt}\right)_{\text{coll}} - \left(\frac{dQ_h}{dt}\right)_{\text{evap}}, \quad (13b)$$

$$\frac{dq}{dt} = \frac{dq_s}{dt} + \left[\frac{(q_s - q)}{dt}, \frac{Q_c}{dt} \right]_{\text{min}} + \left(\frac{dQ_h}{dt}\right)_{\text{evap}}, \quad (14)$$

where $dq_s/dt = 0$ when $q < q_e$, and $dq_s/dt \neq 0$ when $q = q_e$.

e. Entrainment

The standard entrainment rate μ , updraft radius R assumption used in models of this type is used here, namely

$$\mu = \left(\frac{1}{M}\right) \frac{dM}{dz} = \frac{0.2}{R} \text{ [m}^{-1}\text{]}.$$

For the calculations using the hypothetical sounding in the next section, the entrainment rate was assumed equal to zero. For the actual case studies, the entrainment rate given above was used with the observed cloud base radius.

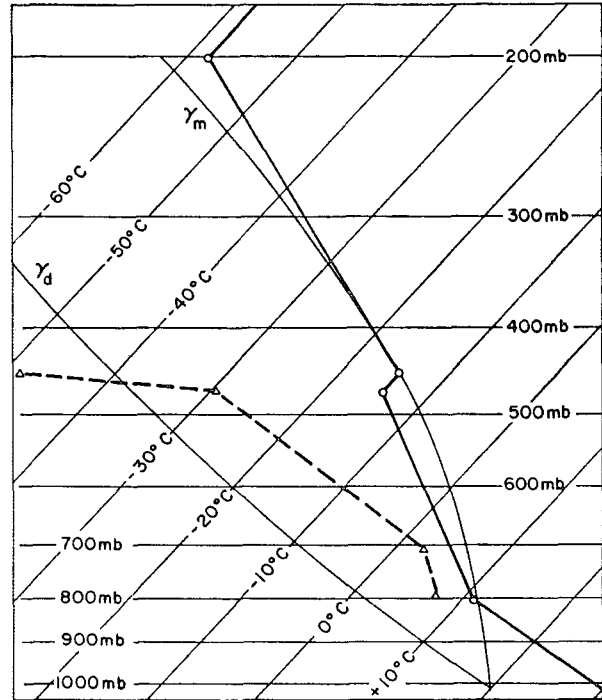


FIG. 1. Sounding used for the initial calculations. Heavy solid line with open circles represents the free-air temperature sounding. Heavy dashed line with open triangles represents the dew-point temperature sounding. The thin solid lines labeled γ_d and γ_m represent the dry and moist adiabatic lapse rates, respectively.

3. Results

Eqs. (4), (6), (13) and (14) were broken into partials of the form $d/dt = \partial/\partial t + w\partial/\partial z$, digitized, and coded in Fortran IV for use on an IBM 360 Model 67. The space derivatives were digitized by upstream space differencing using a vertical grid spacing of 200 m. The time derivatives were digitized by forward time integration using a variable time step according to the linear stability criterion

$$w(\Delta t/\Delta Z) \leq 1,$$

where the vertical velocity used was the maximum vertical velocity in the profile computed at the end of the previous time step. Using this system with all arithmetic done in double precision and a vertical grid interval of 200 m, the program requires 77,000 bytes of core storage and approximately 50 sec of CPU time for 60 min of cloud time for a 7-km deep cloud.

The sounding used for the first set of calculations is shown in Fig. 1. The isothermal layer from 470–450 mb prevents convection from breaking into the less stable layer aloft unless artificial ice nucleation is hypothesized. This is the type of environmental sounding which leads to explosive vertical growth due to seeding. The initial impulse needed to start the calculations is a vertical triangle wave temperature curve with an amplitude of 0.5C and a zero-to-zero half-wavelength of 1.6 km (8 grid intervals) starting from cloud base. The air

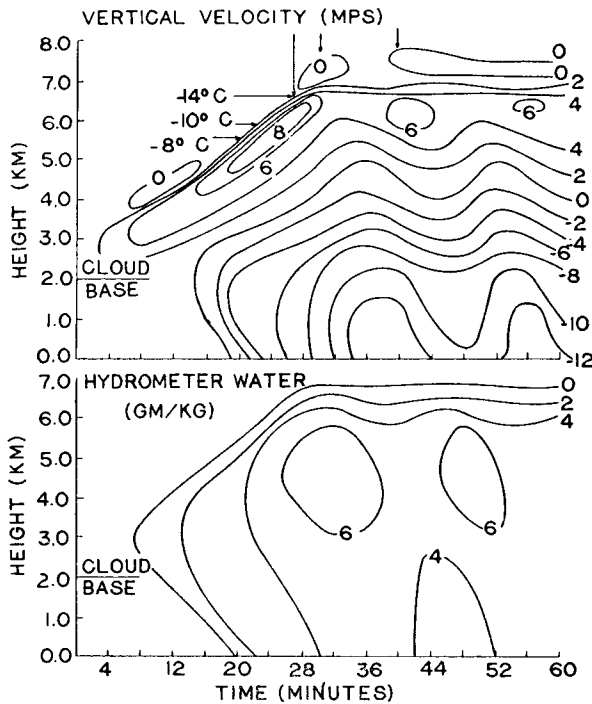


FIG. 2. Time-height cross sections calculated with the cloud microphysics parameters suggested by Kessler *et al.*, $K' = 0.001$, $a = 0.5 \text{ gm kg}^{-1}$, $N_0 = 10^7 \text{ m}^{-3}$, $E = 1$. The horizontal arrows in the upper figure show the levels of several potential seeding temperatures; the vertical arrows show the time of several potential seeding times.

is assumed to be just saturated through this 1.6-km depth.

For all of the calculations to be discussed here, the hydrometeor evaporation parametrization was not used. Calculations other than those discussed here showed that the hydrometeor evaporation only affected the sub-cloud part of the calculation (Weinstein, 1968).

a. Sensitivity analysis

Fig. 2 shows the time-height cross sections of vertical velocity (m sec^{-1}) and hydrometeor water (gm kg^{-1}) for a calculation using the values of the cloud microphysics parameters, K' , a and K'' , suggested by Kessler *et al.* This figure shows the same periodic oscillations that were found by Srivastava (1967) when he ran his calculations on the decay stage of an already developed cloud.

One of the advantages of the parametrization approach is that it allows the parameters to be varied over wide limits in order to determine the effects of each of the processes being parametrized. In this way, the important phenomena can be isolated and the research can be focused upon these processes alone. The parameters, K' , a and K'' (a combination of $6.94 \times 10^{-4} N_0^{-0.125} E$) that Kessler *et al.* derived will be varied over wide limits to see how they affect the calculations.

Before showing the effects of varying these constants, an analysis will be given of their physical meaning.

The expression shown in (8) can be rewritten as

$$\frac{d(Q_c - a)}{dt} = -K'(Q_c - a), \quad (15)$$

where a is the threshold of cloud water content, which does not vary with time. Eq. (15) can be rewritten as

$$\frac{1}{(Q_c - a)} d(Q_c - a) = -K' dt. \quad (16)$$

Integration of (16) from time zero to time t yields

$$\frac{(Q_c - a)_t}{(Q_c - a)_0} = \exp(-K't), \quad (17)$$

where the subscripts represent the cloud water contents at time zero and at time t .

Thus, K' is a time constant, such that it takes $1/K'$ seconds for the initial cloud water content excess over the threshold to be reduced to $1/e$ of its original value before conversion started. With $K' = 0.001 \text{ sec}^{-1}$, the time $t \approx 17 \text{ min}$. Increasing (decreasing) K' by an order of magnitude, decreases (increases) the half-life by one order of magnitude.

The second parameter in the conversion term of (15) is the threshold of cloud water, a . The cloud water content has to build up to this value before conversion can occur. A small value for a means that hydrometeors can be produced very rapidly from a small number of cloud droplets. A large value for a means that there is something inhibiting the production of hydrometeors. Varying the threshold from 0.0 to 6.0 gm kg^{-1} covers the possible range with the present hypothetical sounding, as the latter value of liquid water content is approximately the maximum amount of water generated by the cloud.

Table 1 shows the results of the sensitivity analysis in which K' was varied from 0.01 – 0.0001 sec^{-1} and the threshold a from 0.0 – 6.0 gm kg^{-1} . The first effect to be noted here is that the intensity of the cloud circulation, maximum vertical velocity, and the cloud top height were relatively insensitive to changes in the conversion term. The only cloud dynamics effect of conversion is in the periodicity of the cloud. This effect could not easily be shown in the table, but the effect was to make the cloud assume progressively a more steady state as the conversion rate was decreased and the threshold was increased.

The next result in Table 1 is that the rainfall characteristics are strongly dependent upon the constants in the conversion term. As less conversion is allowed to occur, less rain is produced, and rain that is produced arrives at the ground later in the lifetime of the cloud. The time and height of the first hydrometeor-water

accumulation zone are likewise functions of the time and rate of conversion.

The most important result displayed in Table 1 is the relative importance of the conversion rate and the threshold of cloud water, the latter being far more important than the former. Variation of the rate of conversion over two orders of magnitude, well beyond the natural variation in the atmosphere, and well beyond what might be obtained through cloud modification, generally produced <10% difference in any of the parameters shown in the table. Changes in the threshold of cloud water which could be imagined to occur in the atmosphere, and which could be modified, produced significant changes in the rainfall characteristics.

The physical interpretation of the collection rate, K'' , can be understood better by rewriting Eq. (11) as

$$\frac{dQ_h}{dt} = \frac{-dQ_c}{dt} = K'' \rho^{-0.875} Q_c Q_h^{0.875},$$

where $K'' = 6.96 \times 10^{-4} \mathcal{E} N_0^{0.125}$.

Changing the collection rate K'' by an order of magnitude around the value suggested by Kessler is equivalent to changing the collection efficiency \mathcal{E} by a like amount, or changing the number of drops for the small droplets, N_0 , by eight orders of magnitude either way, or any combination of the two. Since N_0 is raised to the 1/8th power in the equation for the collection rate, the variations in K'' have more physical meaning when they are considered as changes in the collection efficiency. For Kessler's suggested value of 0.0052 for K'' , \mathcal{E} was set equal to 1. Varying the mean collection efficiency from 0.1-10 more than covers the possible range in the atmosphere.

Table 2 shows the results of a sensitivity analysis in which the conversion rate K' and the collection rate K'' were varied over two orders of magnitude, one order of magnitude on either side of the value suggested by Kessler. The differences are far less dramatic than was the case in the conversion sensitivity analysis. The conversion and collection rates have about equal importance, and it is only when each is made quite small that the ultimate rainfall characteristics change drastically.

b. Freezing

Fig. 3 shows the time-height cross sections of vertical velocity and hydrometeor water content for a calculation that allowed freezing to occur at -8C , the temperature most generally accepted as the ice nucleation temperature of silver iodide. It can be seen that the cloud grew 3 km higher and its internal parameters, such as vertical velocity, were all greater than the cloud in which freezing was not allowed to occur (Fig. 2). This is the same result that Davis (1965) obtained with the same environmental sounding. The reason that the cloud grew higher, and that its internal parameters were

TABLE 1. Sensitivity analysis of the conversion rate K' vs the threshold of cloud water content a . The collection rate $K'' = 0.0052 \text{ sec}^{-1}$.

K' (sec^{-1})	a (gm kg^{-1})	Rain (inches)	Rain begins (min)	Height of 1st Q_h (km)	Time of 1st Q_h (min)	Max. w (m sec^{-1})	Cloud top (km)
10^{-2}	0.5	5.06	18	3.0	6	9.3	7.0
	2.0	4.61	26	3.5	10	10.2	7.0
	4.0	2.98	38	4.6	20	8.7	7.0
	6.0	0.53	52	5.8	28	10.1	7.4
10^{-3}	0.0	5.22	18	3.1	8	9.7	7.0
	0.5	5.09	20	3.1	8	9.5	7.0
	1.0	4.83	22	3.3	10	9.7	7.0
	2.0	4.35	28	3.6	12	9.9	7.0
	3.0	3.77	32	4.0	16	9.1	7.0
	4.0	2.78	40	4.7	22	9.1	6.8
10^{-4}	5.0	2.13	46	5.4	26	9.6	7.2
	6.0	0.34	52	6.0	30	10.2	7.4
	0.5	4.79	24	3.1	10	9.6	7.0
	2.0	4.15	30	3.8	14	9.4	7.0
	4.0	2.57	40	4.7	22	9.3	7.0
	6.0	0.05	52	5.9	30	10.3	7.4

all increased, is that the frozen cloud had an added energy source, viz., the latent heat of fusion and sublimation. In this environment, the extra energy allowed the cloud to clear the temperature inversion at 470 mb and grow up into the less stable layer aloft.

There is some question as to the actual activation temperature of various seeding agents. Silver iodide was originally thought to have an activation temperature of -4C . Later it became obvious that silver iodide rarely is activated at temperatures higher than -8C . It is now clear that the activation temperature of this seeding agent is a function of the size and purity of the crystals. There is some evidence to show that the activation temperature of silver iodide is lowered to well below -8C if the particles are made wet upon passing through the warm layers in the cloud. Manufacturers of silver iodide flares have been able to adjust the flare so that the material can be active at different temperatures.

TABLE 2. Sensitivity analysis of the conversion rate K' vs the collection rate K'' . The threshold cloud water content $a = 0.5 \text{ gm kg}^{-1}$.

K' (sec^{-1})	K'' (sec^{-1})	Rain (inches)	Rain begins (min)	Height of 1st Q_h (km)	Time of 1st Q_h (min)	Max. w (m sec^{-1})	Cloud top (km)
10^{-2}	0.052	5.30	16	2.9	6	9.3	7.0
	0.0052	5.06	18	3.0	6	9.3	7.0
	0.00052	4.78	18	3.0	6	8.7	6.8
10^{-3}	0.052	5.28	16	3.1	7	9.4	7.0
	0.0052	5.09	20	3.1	8	9.5	7.0
	0.00052	4.41	22	3.2	8	8.7	6.6
10^{-4}	0.052	5.30	18	3.2	8	9.6	7.0
	0.0052	4.79	24	3.3	10	9.6	7.0
	0.00052	1.14	30	3.7	14	8.9	7.0

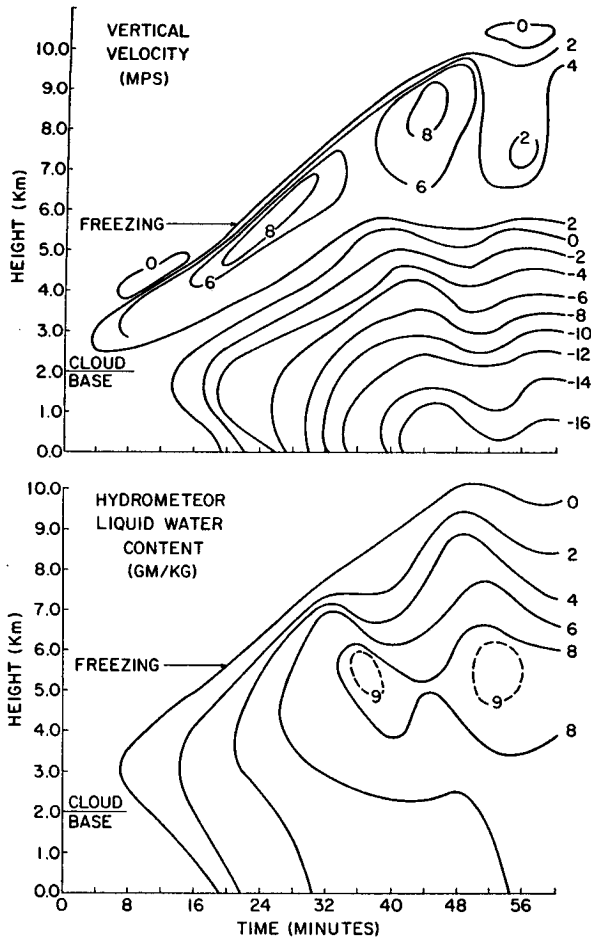


FIG. 3. Time-height cross sections with freezing at -8°C . The horizontal arrows show the time and height of freezing.

An important application of the model is the calculation of the optimum activation temperature of a seeding agent. Fig. 4 shows the per cent increases of cloud-top height and rainfall that could be obtained from freezing the supercooled water at different temperatures for the hypothetical sounding used in the previous calculations. The percentages are based upon the calculation carried out without simulating freezing (cloud-top temperature of -18°C). It can be seen that there is a distinct difference between the shape of the cloud-top and rainfall curves. If seeding effectiveness evaluations were made on the basis of increases of cloud-top height alone, one could conclude that as long as the activation temperature of the material was warmer than -12°C , it really would not make much difference what the freezing temperature actually was. The rainfall curve, on the other hand, shows quite clearly that as the freezing temperature is progressively raised, the rainfall increases become progressively greater up to -4°C . In fact, the rainfall increase for a freezing temperature of -4°C was almost three times that for a freezing temperature of -8°C . The curves, of course, terminate at a tempera-

ture of 0°C as it is physically impossible to have freezing at temperatures $>0^{\circ}\text{C}$.

The reason for the differences between the cloud-top height and rainfall curves can be partially explained by referring back to Fig. 2. The horizontal arrows indicate the levels of the freezing temperature used to construct Fig. 4. As the freezing temperature is progressively raised, the level in the cloud where the greatest amount of extra heat is liberated is progressively lowered. The time-height cross sections from which Fig. 4 was constructed showed that when a lot of heat was liberated near the top of the cloud, the top tended to become somewhat separated from the interior of the cloud. Freezing near the top of the cloud provided a secondary heat source which led to a local acceleration of the cloud top. Since the initial balance level was near the top of the cloud, the local acceleration simply pushed this balance level higher, without materially increasing condensation. When the freezing occurred lower in the cloud, where the change in saturated mixing ratio with height was greater, the local increase in vertical velocity produced increased condensation, rather than simply moving the water higher in the cloud. The increased condensation, or sublimation after freezing has occurred, combined with the buoyant acceleration occurring well below the balance level, caused the hydrometeor water maximum to remain attached to the main body of the cloud.

In this calculation, the freezing was allowed to occur as soon as any liquid water reached the specified ice nucleation temperature. It could be argued that with this type of freezing some heat must always be liberated right at cloud top since the cloud top is always the first part of the cloud to reach the ice nucleation temperature. A look at Fig. 2 shows that $\partial Q_h/\partial t$ at the ice nucleation temperature levels is large, and thus while the first heat that is due to freezing is liberated at the cloud top in all cases, the *greatest* amount of heat is liberated well down into the cloud when the warm ice nucleation

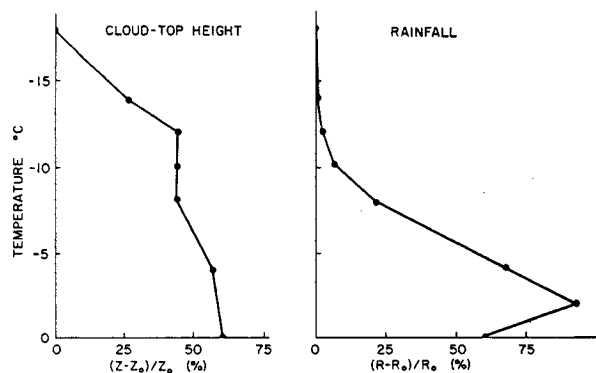


FIG. 4. Potential percentage increases in cloud-top height and rainfall due to seeding as a function of temperature, where Z_0 and R_0 are the cloud-top height and rainfall, respectively, that were computed without simulating freezing.

temperatures are used. It should also be pointed out that the warmer ice nucleation temperatures spread the heat out over a deeper layer than do the colder temperatures.

If one could specify the activation temperature of a seeding material, the next question to be answered is: When should the seeding be done? Fig. 5 shows the percentage increases in cloud-top height and rainfall vs time of freezing for the same sounding. For these calculations, the freezing temperature was -8°C . The times of particular interest are 25 and 30 min. The former was the time when the cloud was undergoing its greatest vertical acceleration without freezing. The latter time was when the cloud had stored the greatest amount of liquid water, and thus its vertical growth had leveled off. The calculations show that the best time to seed a cloud is sufficiently early to allow the material to be activated as the cloud is undergoing its greatest vertical growth. Seeding it at any other time causes some of the energy realized from freezing to be spent in overcoming the natural decay of the cloud. A second reason for the lack of success obtained from freezing at 30 min is that the sudden shock of freezing too much water simply accelerated the updraft. As this happened, a situation occurred similar to that which occurred when freezing was accomplished too near the top of the cloud, i.e., the water accumulation region of the cloud was simply moved higher up.

c. Case Study of 25 July 1967

During the summer of 1967, the author was a member of the Arizona Modification Research Project. The aim of this program was to demonstrate the thermodynamic instability hypothesis for seeding isolated cumuli [see

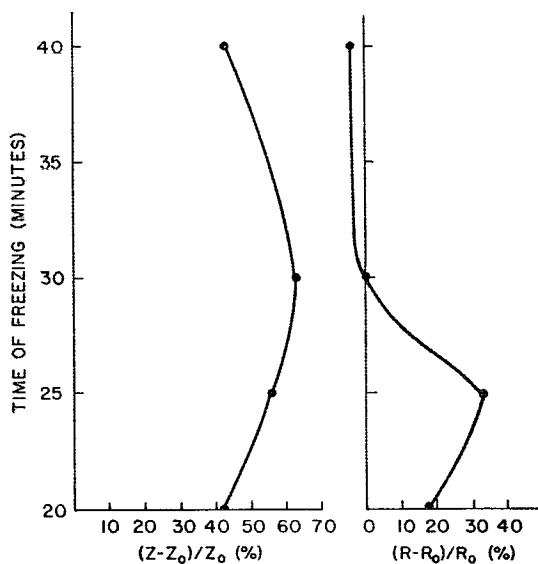


FIG. 5. Same as Fig. 4 except as a function of time for a freezing temperature of -8°C .

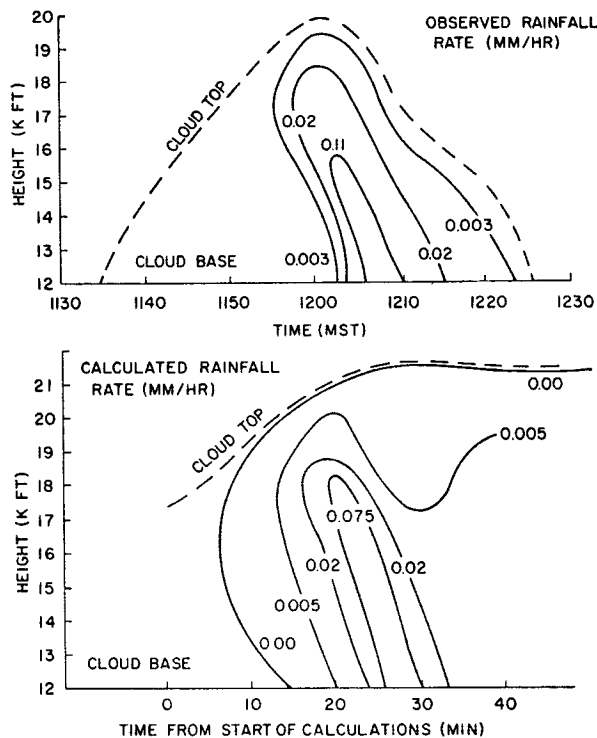


FIG. 6. Observed and calculated cross sections for the control cloud on 25 July 1967.

Weinstein and MacCready (1969) for a description of the program]. As part of the evaluation of the test results, time-height cross sections of radar rainfall rate in the core of the test clouds were constructed. In this section, the calculated time-height cross sections of rainfall rate will be compared with observed cross sections for two of the clouds.

The observations to be used were taken on 25 July 1967. The sounding on that day was similar to the sounding used for the other test cases; a 1.0-km radius cloud would experience explosive vertical growth due to seeding.

Fig. 6 shows the observed and calculated time-height cross sections of rainfall rate for the non-seeded cloud. The observed values were determined by means of the radar reflectivity factor, while the calculated values were obtained from a relationship given by Marshall and Palmer (1948), i.e.,

$$M = 74R^{0.88},$$

where M is the liquid water content³ Q_h (mg m^{-3}) and R the rainfall rate (mm hr^{-1}). It can be seen that the model reproduced the dominant feature of the cloud, viz., the main rain core. The observed rainfall rates were recorded only above cloud base, so this is the only portion of the calculated cross section shown.

³ Actually Q_h has units of gm kg^{-1} , but the density of air can be taken to be 1 kg m^{-3} to the accuracy needed here.

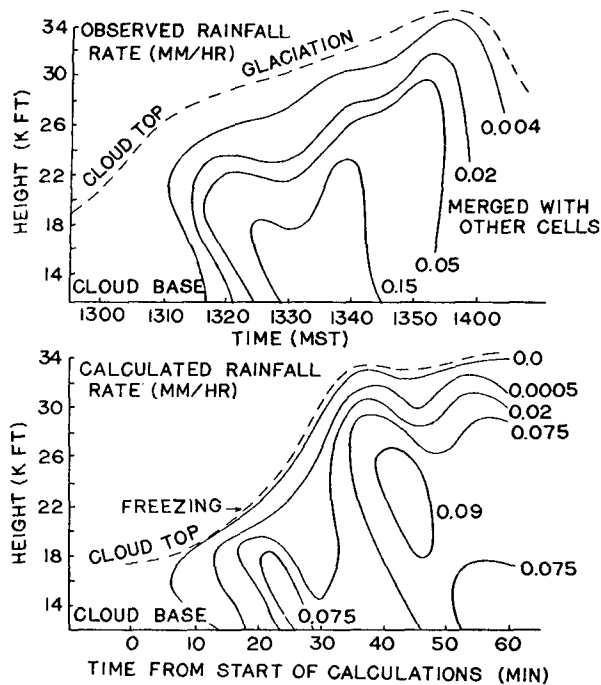


FIG. 7. Observed and calculated cross sections for the seeded cloud on 25 July 1967.

Fig. 7 shows similar cross sections for the seeded cloud. The seeding was responsible for the production of a second rain shaft which the model calculations clearly reproduced. Freezing was allowed to occur at -8°C at the time when the first liquid water reached the freezing level. It should be noted that the freezing occurred in the calculated cross section at the same time that glaciation was observed in the real cloud. This indicates that the time of freezing used in the calculations was correct.

4. Summary and conclusions

Cloud microphysical parametrizations are combined with the dynamical and thermodynamical calculations routinely used to simulate cumulus clouds, to develop a one-dimensional, time-dependent model. The calculations without freezing show the cloud to undergo damped periodic oscillations in time. This type of cloud-top growth is commonly observed in cumuli and has been calculated by others (Srivastava, 1967).

The results of the sensitivity analysis carried out on the microphysical parameters showed that one of the parameters, the conversion threshold, is an important enough parameter to be investigated further. The conversion and collection rates do not appear to warrant further detail as they do not affect the final calculations much. An improvement on the conversion parametrization has been proposed by Berry (1968). This new form no longer requires a threshold cloud water content but rather it uses more fundamental properties of the

droplet and spectrum; namely, the initial number of droplets cm^{-3} and the relative dispersion of the size distribution. This new form should be subjected to a similar sensitivity analysis as has been presented here for Kessler's form.

In the original studies concerned with the dynamics of cumuli only, it was sufficient to show that the cloud-top height of an isolated cumulus cloud could be increased by seeding. Now that the dynamics are better understood, it is necessary to optimize seeding procedures in order to increase the rainfall as much as possible. The freezing calculations showed that cloud-top height increases do not necessarily have a one-to-one correspondence with rainfall increases. Thus, cloud-top height alone should not be used to evaluate the effectiveness of seeding on rainfall.

It was further shown that the activation temperature of the seeding material and the time of freezing are crucial parameters in increasing the rainfall. The calculations showed that if a seeding material has an activation temperature of -10°C instead of the generally accepted -8°C for silver iodide, the increase in rainfall reaching the ground is less than would be assumed from cloud-top height measurements. This result points up the need for more precise measurements of the activation temperatures of seeding agents and for studies of the conditions under which the activation temperature can be altered.

The calculations showed that if the seeding were done at the wrong time in the lifetime of the cloud, the rainfall could actually be reduced while the cloud-top height could show an increase. The results of these calculations indicated that the seeding should be done so that it takes effect during the growing stage of the cloud's lifetime.

It should be noted that both of the above results are for the particular sounding chosen. While this is a typical sounding representative of favorable seeding conditions, more calculations with other soundings will be needed before any generalizations can be made and before seeding procedures can be optimized.

The parametrization used in the model was derived for the warm phase. There are important differences between the particle size distribution, the terminal velocity, and the collection efficiency of raindrops and ice crystals. There are also significant differences between the conversion process in water and ice clouds and in all-water clouds. The parametrization is being worked out for the transformation of water from hydrometeors to ice particles and graupel in order to represent the ice phase more realistically.

Acknowledgments. The work reported upon here was done while the author was at The Pennsylvania State University working with Drs. L. G. Davis and C. L. Hosler. Their guidance in the development of the model and the interpretation of the results is greatly appreciated. The work at Pennsylvania State University was

sponsored by the National Science Foundation under Grant GA-777.

The model development was immeasurably aided by the author's experiences as part of the Arizona Modification Research Project in Flagstaff, Ariz., during the summers of 1966 and 1967. This project was run by Meteorology Research, Inc., and was sponsored by the Bureau of Reclamation under Contract 14-06-D-5589. This paper was written at MRI under this same sponsorship.

REFERENCES

- Austin, J. M., and A. Fleisher, 1948: A thermodynamic analysis of cumulus convection. *J. Meteor.*, **5**, 240-243.
- Berry, E. X., 1968: A parameterization of the collection of cloud drops. *Proc. Intern. Conf. Cloud Physics*, Toronto, Canada, 111-114.
- Davis, L. G., 1965: Alterations of buoyancy in cumuli Ph.D. thesis, The Pennsylvania State University, University Park, 98 pp.
- Hosler, C. L., L. G. Davis and D. R. Booker, 1963: Modification of convective systems by terrain with local relief of several hundred meters. *Z. Angew. Math. Phys.*, **14**, 410-419.
- Kessler, E., III, P. J. Feteris, E. A. Newberg and G. Wickham, 1962-64: Relationship between tropical precipitation and kinematic cloud models. Prog. Repts. 1-5, The Travelers Research Center, Inc., Hartford, Conn., Cont. DA-36-039-SC89099. (Available from DDC, Cameron Station, Alexandria, Va. 22314, as AD 286 737, AD 296 036, AD 402 766, AD 424 993, AD 437 817).
- Marshall, J. S., and W. McK. Palmer, 1948: The distribution of raindrops with size. *J. Meteor.*, **5**, 165-166.
- Simpson, J., R. H. Simpson, D. A. Andrews and M. A. Eaton, 1965: Experimental cumulus dynamics. *Rev. Geophys.*, **3**, 387-431.
- Srivastava, R. C., 1967: A study of the effects of precipitation on cumulus dynamics. *J. Atmos. Sci.*, **24**, 36-45.
- Weinstein, A. I., 1968: A numerical model of cumulus dynamics and microphysics. Ph.D. thesis, The Pennsylvania State University, University Park., 75 pp.
- , and P. B. MacCready, Jr., 1969: An isolated cumulus cloud modification project. *J. Appl. Meteor.*, **8**, 936-947.